USB Proceedings

2014 International Conference on Electrical Machines (ICEM)

Andel`s Hotel Berlin
Berlin, Germany
02 - 05 September, 2014

Sponsored by

The Institute of Electrical and Electronics Engineers (IEEE)
IEEE Industrial Electronics Society (IES)

Co-sponsored by

ETG - Power Engineering Society withing VDI

Impact of the load in the detection of bearing faults by using the stator current in PMSM's

Christelle Piantsop Mbo'o, Thomas Herold and Kay Hameyer
Institute of Electrical Machines (IEM)
www.iem.rwth-aachen.de
RWTH Aachen University
Schinkelstrasse 4, 52062 Aachen, Germany
Email: christelle.piantsop@iem.rwth-aachen.de

***Abstract*—Many mechanical faults in industrial processes are related to bearing damage, which can be detected by vibration analysis. This approach may be expensive due to the cost of sensors. Therefore, studies are performed in order to use the stator current to detect bearing damage. This study is to investigate the impact of the load in the bearing damage detection by using the stator current. A diagnostic index is developed and evaluated for vibration signals measured from a healthy and a damaged bearing. Afterwards, the validated index is applied to the stator current of a permanent magnet synchronous machine measured with a healthy and a damaged bearing at different loads. The results show that, the damaged bearing can be differentiated from the healthy bearing by using the proposed index with the signal of the vibration or the stator current. However, the detection by the stator current is strongly dependent on the radial force of the bearing.**

***Keywords*—bearing damage, fault detection, stator current, permanent magnet synchronous machine, spectral analysis, vibration analysis**

I. Nomenclature

f_{outer}, f_{inner}	characteristic fault frequency
f_{ball}, f_{cage}	related to the bearing parts
f_{acc}	structural vibration fault frequency
f_c	stator current fault frequency
f_{rm}	mechanical rotational frequency
f_{el}	electric supply frequency
N_{ball}	number of balls or cylindrical rollers
D_{ball}	diameter of balls or cylindrical rollers
D_{cage}	diameter of cage
β	contact angle of balls or cylindrical rollers
k_0	fundamental order of the bearing outer race damage
k_c	fault order of the current related to the mechanical rotational frequency
ν	harmonic of current
Ps	signal power
T_N	nominal torque

II. Introduction

Increasing system reliability is an important issue for many applications. Therefore, condition monitoring systems are permanently being improved with respect to the early detection of anomalies in the electrical or mechanical parts of a drive train. These are performed in order to avoid a breakdown of the entire drive system. The most common mechanical faults in industrial processes are related to the bearing damages [1], [2]. These are detected essentially by vibration analysis with different detection methods [3]–[5]. This monitoring technique is expensive and requires a challenging mechanical construction depending on the number of used accelerometers and the kind of bearing. For this reason, an alternative detection approach is studied in [6]–[19]. There, the stator current signal of the permanent magnet synchronous machine (PMSM) as well as the induction machine is used to detect bearing damage in the drive train. The objective of this method is to utilize the embedded current sensors of the controller for faults detection as well.

A bearing damage causes characteristic frequencies in the structural vibration spectrum, which depend on the mechanical rotational speed and the kind of bearing fault. Bearing damages lead to torque pulsations resulting in speed fluctuations, which induce oscillations in the motor current with the characteristic frequencies. These fault frequencies depend on the electric supply frequency and the vibration frequencies. In this paper, a diagnostic index for the detection of bearing damages is developed. The index assesses the energy of the characteristic frequencies and is evaluated by using the measured data of the vibration from a healthy bearing and a bearing with damage in the outer race. Afterwards, this procedure is applied to the stator current signal of a PMSM and the generated fault index is evaluated at different load operations in order to investigate their influence on the fault detection. The proposed method is not based on the vibration transferred into the air gap of the machine but on the torque feedback of the bearing damage.

This paper is organized as follows: a short overview of bearing damages is given in section III, in which the used bearing for the study and its damage are presented. Section IV describes the test bench and the test procedure, while the implementation of the fault index is described in section V. Furthermore, the index is applied to the vibration signal in section VI and the stator current signal in section VII. Finally, the work is summarized and concluded in section VIII.

978-1-4799-4775-1/14/$31.00 ©2014 IEEE

III. Bearing damages

Rolling bearings are usually used to guide and to support the shaft in rotating machines. They consist of an inner and outer race, which are separated by rolling elements such

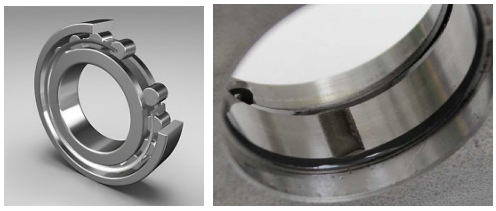

Fig. 1. Cylindrical-roller bearing (left) and bearing damage in outer race (right)

as balls or cylindrical rollers. The rollers are integrated in a cage to avoid contact. Rolling bearings can damaged by different causes so that local or distributed defects occur. Distributed defects due to generalized roughness [20] affect the whole region of the bearing and cannot be recognized through particular frequencies compared to local defects. Hence, only the local defect is discussed in this paper. This can be classified in function of the affected part of the bearing such as: inner race fault, outer race fault, cage fault and ball fault. These faults cause characteristic frequencies in the vibration spectrum, which depend on the geometry of the rolling elements and the mechanical rotational frequency f_{rm}. The characteristic frequency of each fault type are described in [14] and [20] as follows:

Outer race defect:

$$f_{outer} = \frac{N_{ball}}{2} \cdot f_{rm} \cdot (1 - \frac{D_{ball}}{D_{cage}} \cos\beta) \tag{1}$$

Inner race defect:

$$f_{inner} = \frac{N_{ball}}{2} \cdot f_{rm} \cdot (1 + \frac{D_{ball}}{D_{cage}} \cos\beta) \tag{2}$$

Ball defect:

$$f_{ball} = \frac{D_{cage}}{2 \cdot D_{ball}} \cdot f_{rm} \cdot (1 - \frac{D_{ball}^2}{D_{cage}^2} \cos\beta^2) \tag{3}$$

Cage defect:

$$f_{cage} = \frac{1}{2} \cdot f_{rm} \cdot (1 - \frac{D_{ball}}{D_{cage}} \cos\beta) \tag{4}$$

whereas N_{ball} is the number of balls or cylindrical rollers, β the contact angle of the balls, D_{ball} the ball or roller diameter and D_{cage} the cage diameter, also known as the ball or roller pitch diameter. In the following study two cylindrical-roller bearings (Fig. 1, left) are used: a healthy bearing and a bearing with an artificial damage in the outer race (Fig. 1, right). The inner side of the outer race is wire eroded. The wire has a diameter of $8\,\mathrm{mm}$ and produces a damage point with a width of $2.82\,\mathrm{mm}$. The bearing parameter is given in the table I.

According to [2], the contact angle is $0°$ for cylindrical-roller bearing. Therefore, the characteristic frequency is reduced to

$$f_{outer} = \frac{N_{ball}}{2} \cdot f_{rm} \cdot (1 - \frac{D_{ball}}{D_{cage}}). \tag{5}$$

TABLE I. DATA OF THE USED CYLINDRICAL-ROLLER BEARING.

roller diameter D_{ball}	6.5 mm
cage diameter D_{cage}	28.6 mm

TABLE II. DATA OF THE USED MACHINE (RATED VALUES).

PMSM	
pole pair	4
number of phases	3
number of slots	6
power	500 W
current	2.3 A
speed	$3000\,\mathrm{min}^{-1}$
torque	1.6 Nm

Considering the geometry of the bearing and the number of balls, the characteristic frequency of the bearing fault is

$$f_{outer} = 4.25 \cdot f_{rm} \tag{6}$$

and hence the fundamental order of the used bearing in the case of an outer race damage is $k_0 = 4.25$.

IV. TEST PROCEDURE

The test bench consists of a vector-controlled permanent magnet synchronous machine, a magnetic break (load) and a cylindrical-roller bearing in a special test-bench housing. The data of the used machine are given in table II. Fig. 2 shows the schematic setup of the used test bench. A further description is given by [21]. The bearing housing is connected to the motor and the load by shaft couplings and is equipped with accelerometers to measure the vibration in addition. In order to apply an adjustable force to the bearing, a load mechanism is included in the housing of the bearing. The force is measured by a force transducer. The currents, measured within the power source, are used for the machine control, as well as for the bearing fault diagnosis. For the practical experiment two bearings are used: a healthy bearing and a damaged bearing described in section III. The bearing housing has the possibility to adjust the radial force on the bearing up to $5\,\mathrm{kN}$. For this purpose, the bearing outer race must be positioned in such a way that the applied force acts exactly on the damaged area. The performed tests are startup operations with a steady acceleration up to nominal speed by variation of the radial force of the bearing and the load torque.

V. FAULT INDEX

The damage detection is based on an index, which is calculated from a spectral analysis of the vibration or the stator current. Only the expected harmonic orders k of the characteristic frequencies are used for the index calculation. The fundamental order k_0 of the bearing damage outer race was calculated in advance in section III by geometric considerations.

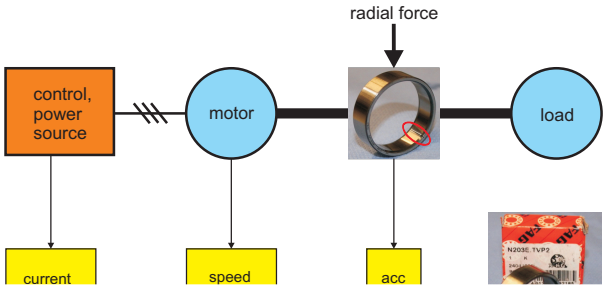

Fig. 2. Schematic setup of the test bench.

The expected signal frequencies for the vibration f_{acc} are a multiple of f_{outer}.

$$\begin{aligned} f_{acc} &= n \cdot f_{outer} = n \cdot k_0 \cdot f_{rm} \\ n &= 1, 2, 3, ... \end{aligned} \tag{7}$$

Due to the fact, that ball bearings support the rotor, any bearing damage causes a radial motion between the rotor and the stator. Additionally, applying a radial force on a damaged bearing causes a rise of the friction torque. This interferes with the load torque and leads to torque pulsations resulting in speed fluctuations. The speed fluctuations, in turn, effect oscillations in the induced voltage that cause oscillations in the motor with the frequencies f_c.

$$\begin{aligned} f_c &= f_{el} \pm n \cdot f_{outer} = f_{el} \pm n \cdot k_0 \cdot f_{rm} \\ n &= 1, 2, 3, ... \end{aligned} \tag{8}$$

The supply frequency can also be expressed as $f_{el} = p \cdot f_{rm}$ with p as the pole pair number. Only the fundamental order is considered in (8). In addition to the fundamental order, other orders occur in the practice in the current spectrum due to unbalance or manufacturing tolerances. These have to be considered for the index calculation. The current harmonics orders are defined as:

$$\begin{aligned} n_{ch} &= \frac{6 \cdot g}{d} + 1 \\ g &= 0, \pm 1, \pm 2, \pm 3, ... \\ d &= 4 \text{ for the used machine.} \end{aligned} \tag{9}$$

The equation (9) give the theoretical current harmonics, which could appear in the stator current spectrum.
For $g = 0 \ldots \pm 5$,
these are $0.5,\ 1,\ 2,\ 2.5,\ 3.5,\ 4,\ 5, 5.5,\ 6.5,\ 7,\ 8$.
Additionally, other orders can occur due to manufacturing tolerances such as non-ideal manufactured rotor components or eccentricity [22].
These are for example:
$0.25,\ 0.5,\ 0.75,\ 1.25,\ 1.5,\ 1.75,\ 2.25,\ 2.5,\ 2.75,\ 3,\ 5,\ 7$.
In order to determine the relevant orders, the machine was run in startup test up to nominal speed, with a healthy bearing and in no load condition. The current spectrum is shown in Fig. 3. The value of the current is indicated by means of the line intensity. The highest value is therefore represented by a white line.
The following orders: $0.5,\ 0.75,\ 1,\ 1.25,\ 2,\ 2.5,\ 3,\ 4,\ 5,\ 7$ occur in the current spectrum.
The significant, not even order, selected for the investigation are: $0.5,\ 0.75,\ 1,\ 1.25,\ 2.5,\ 3,\ 5,\ 7$.
The characteristic frequencies, which occur in the current spectrum is now defined as a function of the current harmonic orders n_{ch}.

$$\begin{aligned} f_c &= n_{ch} \cdot f_{el} + n \cdot k_0 \cdot f_{rm} \\ f_c &= (n_{ch} \cdot p \pm n \cdot k_0) \cdot f_{rm} = k_c \cdot f_{rm} \\ n &= 1, 2, 3, ... \text{ and} \\ n_{ch} &= 0.5,\ 0.75,\ 1,\ 1.25,\ 2.5,\ 3,\ 5,\ 7 \end{aligned} \tag{10}$$

The index can be calculated for each considered harmonic order by integration over the signal power (p_s) in an ordinal cut:

$$a = \int_k p_s(f, k) \mathrm{d}f_{rm}. \tag{11}$$

The fundamental fault order, the significant harmonic orders for the structural vibration and the current have to be pro-

of the bearing dimensions, the fundamental fault order k_0 can vary around its idealized value of 4.25. An occurring slip also effects a decreasing order. Moreover, the spectral

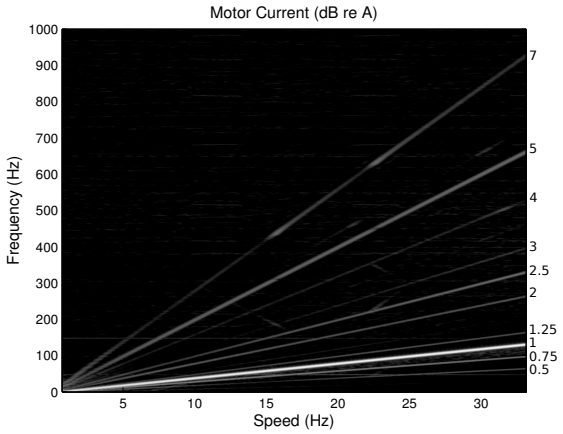

Fig. 3. Current spectrum by healthy bearing - without load torque and radial force.

analysis has some leakage due to increasing speed and is quantized. For this reason, the explicit frequencies are not accessible. Thus, the calculation of the index does not only use the explicit frequencies but also an area around the ordinal cut (e.g. $\pm 1\%$). Due to the quantization, the integral function becomes a summation with a different number of summands for each order. According to that, the sum is divided by this number in order to obtain a normalized comparable signal power of the ordinal cut for each order.

$$idx(f) = \frac{1}{z} \sum_{m=1..z} p_s(f, m) \tag{12}$$

For the comparison of the results, a relative deviation of the index between the healthy and the faulty case is introduced as:

$$\Delta_r(idx, f) = \frac{|idx_{healthy}(f)| - |idx_{faulty}(f)|}{|idx_{healthy}(f)|}. \tag{13}$$

VI. Structural vibration

In this experiment, startup tests up to the nominal speed are performed with the machine. The machine was studied at no load operation. A constant radial force of $5\,\mathrm{kN}$ is applied both to the healthy bearing and to the damaged bearing. The vibration is measured on the housing of the bearing and the fault index is calculated from its spectrogram. Fig. 4 shows the complete spectrogram for both experiments. The value of the surface acceleration is represented by the intensity of the line. Thereby, the white line represents the highest value.
The relevant parts of the spectrogram ($f_{acc} \pm 1\%$ of (7)) is extracted and the first ten fault orders n are shown in Fig. 5. In the faulty case, the fault orders occur with a higher amplitude when compared to the healthy case. The index values for all investigated orders are obtained by applying the index calculation (12) to the extracted spectrogram. These are illustrated in Fig. 6, in which the index signal of the faulty bearing is significantly higher than the index signal of the healthy one. Hence, the developed index by means of the vibration signal allows a good separation between the healthy and the faulty case and is able to be applied to the stator current signal.

Similar to the experiment in the previous section, startup tests up to the nominal speed are performed with the machine at different loads.

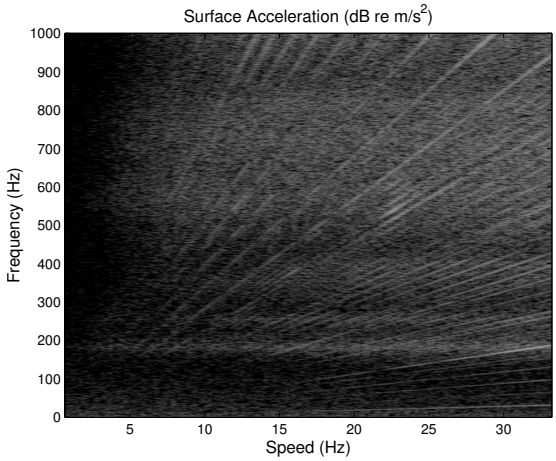

(a) Healthy bearing

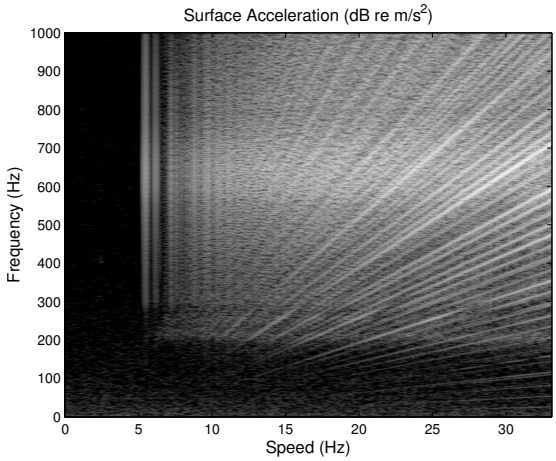

(b) Faulty bearing

Fig. 4. Vibration spectrum by healthy (a) and faulty bearing (b) - radial force 5kN, no load.

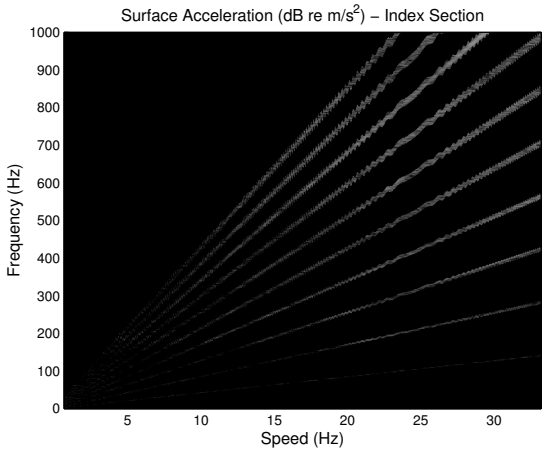

(a) Healthy bearing

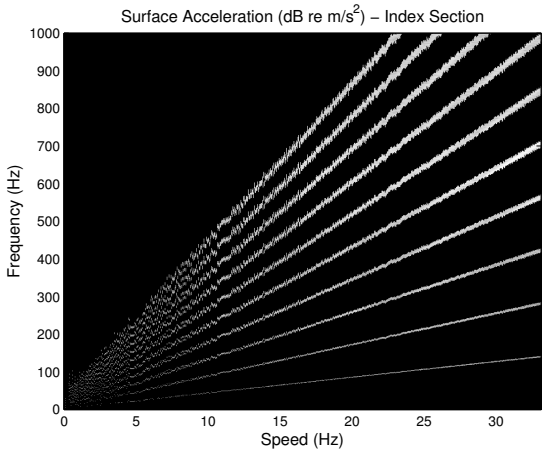

(b) Faulty bearing

Fig. 5. Relevant parts of vibration spectrum by healthy (a) and faulty bearing (b) - radial force 5 kN, no load - index section.

Firstly, a no load operation is performed by a constant radial force of 5 kN. Fig. 7 shows respectively the complete spectrogram of the current signature for the healthy and the faulty bearing. New orders related to the fault can be identified in the spectrogram of the faulty case.

In the following, the change of the index by varying the radial force is studied. For this purpose, the experiment is performed without load and the radial force is increased as follows: 0 kN, 2 kN and 5 kN. The measured stator current signal are spectrally analyzed and the relevant parts of the spectrogram ($f_c \pm 1\%$ of (10)) are extracted in order to evaluate the current index.
For this, significant current harmonic orders such as $n_{ch} = 0.5,\ 0.75,\ 1,\ 1.25,\ 2.5,\ 3,\ 5,\ 7$ are used.
These data are calculated beforehand in section V. By limiting n in (10) to a maximum of 4, the number of considered fault orders is 48. The signal power of the fault orders are extracted from the spectrogram and the corresponding index values are calculated. Fig. 8 shows the index for the extracted orders, respectively by the radial force described above and at no load operation. The fault order on the x-axis is related to k_0: k_c/k_0. As shown in Fig. 8(a), the index values of the healthy and the faulty bearing are similar, when the applied radial force is close to zero ($F = 0$ kN). In contrast to this, the deviation of increased by rising the radial force as observed in Fig. 8(b) and 8(c). A considerable difference is present at the radial force of $F = 5$ kN (Fig. 8(c)). When compared to the fault index of the vibration, the deviation observed on the fault index of the current is smaller. However, there are significant deviations for some orders, which can be used for the fault detection. In addition, in all of the considered radial forces, especially at 2 kN and 5 kN, the index value of three fault orders is smaller in the faulty case than in the healthy case. These fault orders are 0.72th, 1.16th and 4.7th, which coincide with the natural current harmonic: 0.75, 3 and 5 of the machine. These frequency orders should explicitly not

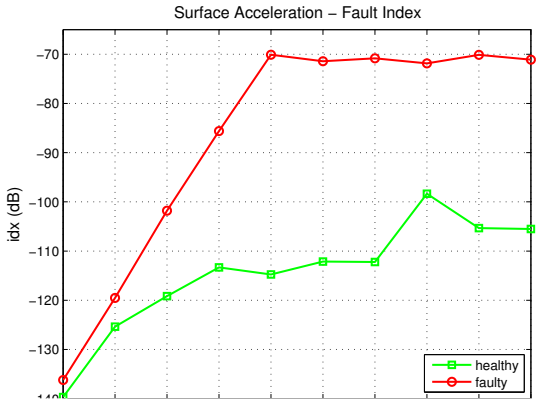

Fig. 6. Vibration index signal of healthy and faulty bearing - 5 kN radial force and no load.

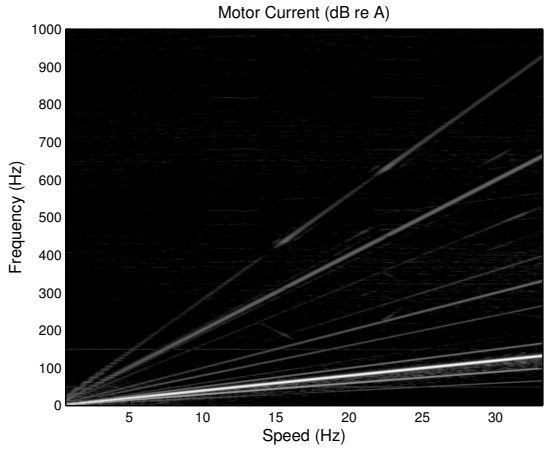

(a) Healthy bearing

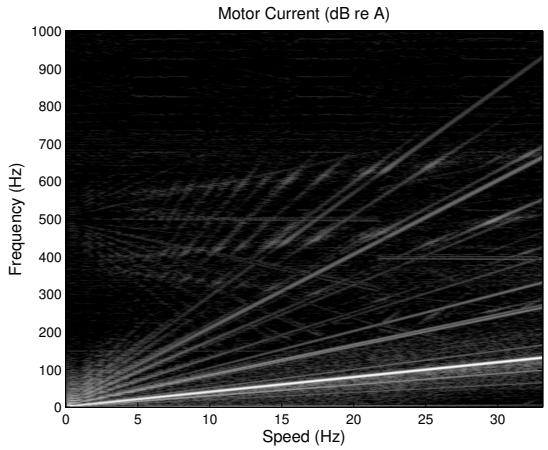

(b) Faulty bearing

Fig. 7. Current spectrum by healthy (a) and faulty bearing (b) - radial force 5 kN, no load.

be used for the fault detection, because the deviation caused by the damaged bearing is masked.

Moreover, the influence of the load torque on the fault detection is investigated. For this, experiments are performed with the following loads: at no load and with 50% of the nominal torque respectively at a radial force of: $F = 0\,\text{kN},\ 2\,\text{kN}$ and $5\,\text{kN}$. In order to compared the results, the relative deviation defined in (13), is calculated by means of the index values obtained from the spectrogram of the stator current signal for all measurements. These are showed in Fig. 9 as a function of the fault orders. The relative deviation in healthy case is zero and is represented as a reference line. Fig. 9(a) illustrated the relative deviation by the radial force $F = 0\,\text{kN}$ respectively at no load and $T = 50\%T_N$. The relative deviation in both cases are similar and very close to the reference line. The maximum deviation is increased of less than 1% at $T = 50\%T_N$. The same behavior is observed in Fig. 9(b) and 9(c), in which the relative deviation are similar at different load torque. A rise of less than 3% is observed by higher load torque. In contrast to this, the deviation of high radial forces is higher as we can see on Fig. 9(b) and 9(c). E.g., the relative deviation has a maximum value of $\Delta_r = 25.52\%$ by the load case $F = 2\,\text{kN},\ T = 50\%T_N$ and $\Delta_r = 47.76\%$ by $F = 5\,\text{kN},\ T = 50\%T_N$, as shown in the table III.

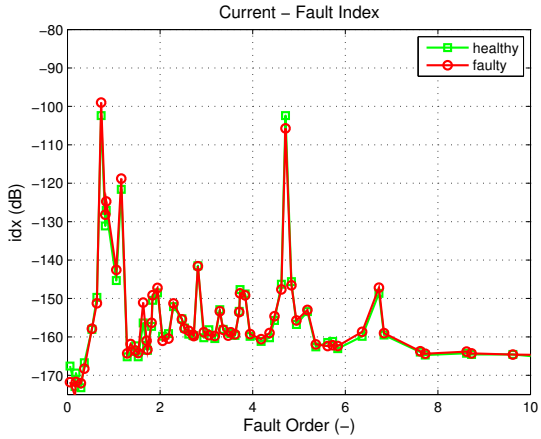

(a) 0 kN radial force, no load

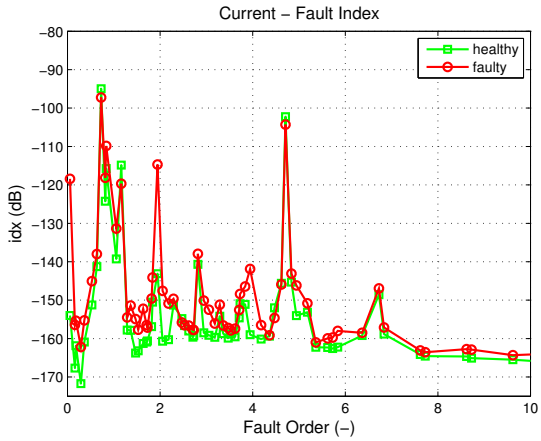

(b) 2 kN radial force, no load

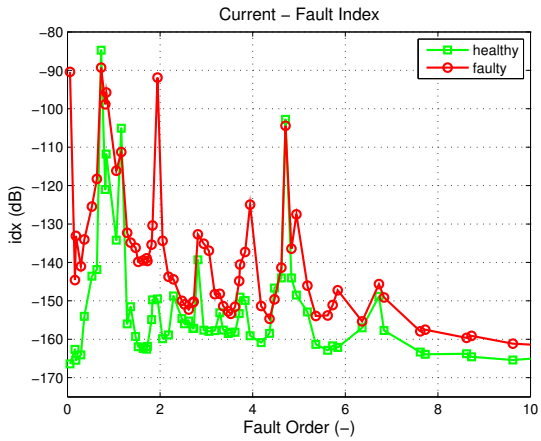

(c) 5 kN radial force, no load

Fig. 8. Current index signal of healthy and faulty bearing - respectively by 0 kN, 2 kN and 5 kN radial force, no load.

considered load operations. Despite the variation of the load torque, the deviation remains similar by the considered radial forces. In conclusion, the relative deviation is not affected from the load torque as from the radial force. The fault detection by radial force close to the value of zero is almost impossible (Fig. 9).

VIII. Summary and Conclusions

In this paper, a bearing damage within an electrical drive train is detected by the analysis of the structural vibration and the stator current of a PMSM. For this purpose, measured data of the vibration were spectrally analyzed of a normalized signal power for selected harmonic orders and a relative deviation of the fault index was introduced for a better comparison of the results. The selected orders

TABLE III. MAXIMAL RELATIVE DEVIATION FOR ALL LOAD OPERATIONS.

Radial force	Load torque: $T_N = 0\,\mathrm{Nm}$	$T_N = 50\%T_N$
$F = 0\,\mathrm{kN}$	$\Delta_r = 3.3\%$	$\Delta_r = 4.07\%$
$F = 2\,\mathrm{kN}$	$\Delta_r = 23.09\%$	$\Delta_r = 25.52\%$
$F = 5\,\mathrm{kN}$	$\Delta_r = 45.68\%$	$\Delta_r = 47.76\%$

were determined beforehand by geometric and physical considerations. The introduced index was applied to the vibrations measured from a healthy and a damaged bearing. The vibration index allows a good separation between the faulty and the healthy case. Then, the methodology behind this index is applied to the stator current spectrum measured by different loads. Thereby, current harmonic orders were precalculated and significant orders were extracted for the index calculation. These depend on the bearing, the location of the damage and the design of the machine. Moreover, the influence of the radial force and the load torque on the fault detection was studied. As a result, a damaged bearing causes an observable signature in the index especially for a high radial force. The radial force has a considerable influence on the fault detection, when compared to the load torque. A load change leads to an insignificant change in the deviation. This is an appreciated behavior, since it makes a diagnosis possible even at different load scenarios. Not all frequencies are suitable for the fault detection. The index deviation at fault orders close to the natural current harmonics are negative or close to zero. Therefore, these should not be considered for the fault detection.

Nevertheless, the algorithm shows promising results. A further signal conditioning can enable a more reliable monitoring, which could help to detect small bearing damages and the damage progress, even at small radial forces.

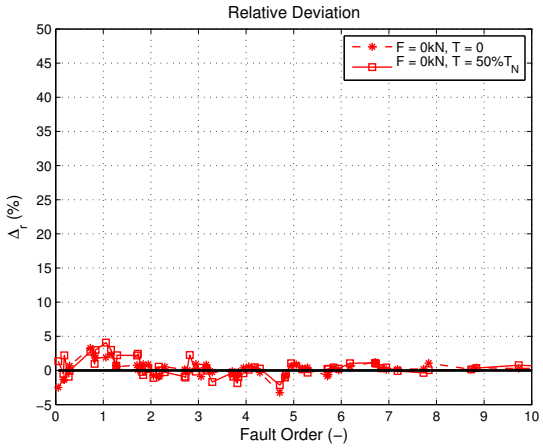

(a) 0 kN radial force, 0% and 50% of nominal torque

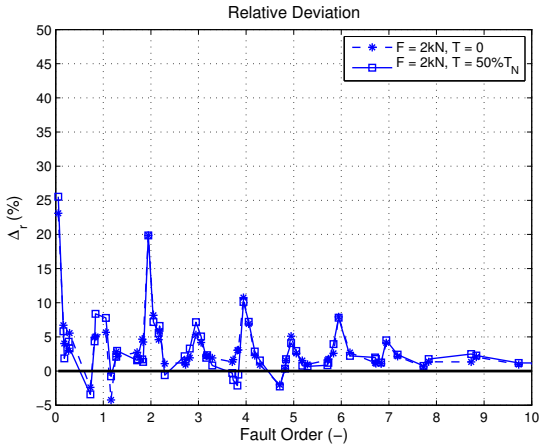

(b) 2 kN radial force, 0% and 50% of nominal torque

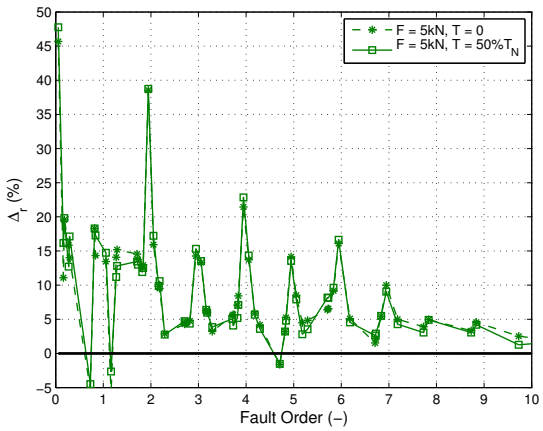

(c) 5 kN radial force, 0% and 50% of nominal torque

Fig. 9. Relative deviation of the index between the healthy and faulty case by all considered load operations.

REFERENCES

[1] Bonnett, A.H.; Yung, C.: "Increased Efficiency Versus Increased Reliability", Industry Applications Magazine, IEEE, vol. 14, no. 1, pp. 29-36, January - February 2008.

[2] P. Tavner, L. Ran, J. Penman and H. Sedding: "Condition monitoring of rotating electrical machines", IET Power and Energy Series, 56, 2008.

[3] Del Vescovo, G.; Paschero, M.; Rizzi, A.; Di Salvo, R. and Mascioli, F.M.F.: "Multi-fault diagnosis of rolling-element bearings in electric machines", XIX International Conference on Electrical Machines, ICEM 2010, pp. 1-6, 6-8 September 2010.

[4] Delgado, M.; Cirrincione, G.; Garcia, A.; Ortega, J. A. and Henao, H.: "A novel condition monitoring scheme for bearing faults based on Curvilinear Component Analysis and hierarchical neural networks", XXth International Conference on Electrical Machines, ICEM 2012, pp. 2472,2478, 2-5 September 2012.

[5] Bediaga, I.; Mendizabal, X.; Arnaiz, A.; Munoa, J.: "Ball bearing damage detection using traditional signal processing algorithms", Instrumentation & Measurement Magazine, IEEE, vol. 16, no. 2, pp. 20 - 25, April 2013.

[6] Schoen, R.R.; Habetler, T.G.; Kamran, F.; Bartfield, R.G.: "Motor bearing damage detection using stator current monitoring", IEEE Transactions on Industry Applications, vol. 31, no. 6, pp. 1274 - 1279, November - December 1995.

[7] Nandi, S.; Toliyat, H.A.; Xiaodong Li: "Condition monitoring and fault diagnosis of electrical motors-a review", IEEE Transactions on Energy Conversion, vol. 20, no. 4, pp. 719-729, December 2005.

[8] Pacas, M.; Villwock, S.; Dietrich, R.: "Bearing damage detection in permanent magnet synchronous machines", IEEE Energy Conversion Congress and Exposition, ECCE 2009, pp. 1098 - 1103, September 2009

for PMSM running under Bearing Damage", Twenty-Fourth Annual IEEE Applied Power Electronics Conference and Exposition, APEC 2009, pp. 951 - 956, 15-19 February 2009.

[10] Ebrahimi, B.M.; Faiz, J.; Araabi, B.N.: "Pattern identification for eccentricity fault diagnosis in permanent magnet synchronous motors using stator current monitoring", Electric Power Applications, IET, vol. 4, no. 6, pp. 418 - 430, July 2010.

[11] Picot, A.; Obeid, Z.; Regnier, J.; Maussion, P.; Poignant, S.; Darnis, O.: "Bearing fault detection in synchronous machine based on the statistical analysis of stator current", IECON 2012 - 38th Annual Conference on IEEE Industrial Electronics Society, pp. 3862 - 3867, 25-28 October 2012.

[12] Rezig, A.; N'Diaye, A.; Mekideche, M. R. and Djerdir, A: "Mod-

Machines, ICEM 2012, pp. 1778 - 1782, 2-5 September 2012.

[13] Obaid, R. R.; Habetler, T. G. and Stack, J. R.: "Stator current analysis for bearing damage detection in induction motors", 4th IEEE International Symposium on Diagnostics for Electric Machines, Power Electronics and Drives, SDEMPED 2003, pp. 182 - 187, 2003.

[14] Blodt, M.; Granjon, P.; Raison, B.; Rostaing, G.: "Models for bearing damage detection in induction motors using stator current monitoring", IEEE International Symposium on Industrial Electronics, vol. 1, pp. 383 - 388, May 2004.

[15] Silva, J. and Cardoso, A. J. M.: "Bearing failures diagnosis in three-phase induction motors by extended Park's vector approach", 31st Annual Conference of IEEE Industrial Electronics Society, IECON 2005, vol. 6, pp. 2591 - 2596, 6-10 November 2005.

[16] Immovilli, F.; Bellini, A.; Rubini, R. and Tassoni, C.: "Diagnosis of Bearing Faults of Induction Machines by Vibration or Current Signals: A Critical Comparison", IEEE Transactions on Industry Applications, vol. 46, pp. 1350 - 1359, 2010.

[17] Immovilli, F.; Cocconcelli, M.; Bellini, A. and Rubini, R.: "Detection of Generalized-Roughness Bearing Fault by Spectral-Kurtosis Energy of Vibration or Current Signals", IEEE Transactions on Industrial Electronics, vol. 56, pp. 4710 - 4717, 2009.

[18] Zhou, W.; Lu, B.; Habetler, T. and Harley, R.: "Incipient Bearing Fault Detection via Motor Stator Current Noise Cancellation Using Wiener Filter", IEEE Transactions on Industry Applications, 2009, vol.45, pp. 1309 - 1317.

[19] Soualhi, A.; Clerc, G.; Razik, H. and Lebaroud, A.: "Fault detection and diagnosis of induction motors based on hidden Markov model", XXth International Conference on Electrical Machines, ICEM 2012, pp. 1693 - 1699, 2-5 September 2012.

[20] Stack, J.R.; Habetler, T.G. and Harley, R.G.: "Fault classification and fault signature production for rolling element bearings in electric machines", 4th IEEE International Symposium on Diagnostics for Electric Machines, Power Electronics and Drives, SDEMPED 2003, pp. 172 - 176, 24-26 August 2003.

[21] Christian Lessmeier, Christelle Piantsop Mbo'o, Isabel Coenen, Detmar Zimmer and Kay Hameyer: "Untersuchung von Bauteilschäden elektrischer Antriebsstränge im Belastungsprüfstand mittels Statorstromanalyse", ANT Journal, Technische Fachzeitschriften der Vereinigten Fachverlage GmbH, vol. 1, pp. 8 - 13, 2012.

[22] Isabel Coenen, Thomas Herold, Christelle Piantsop Mbo'o and Kay Hameyer: "Evaluating the influence of manufacturing tolerances in permanent magnet synchronous machines", The International Journal for Computation and Mathematics in Electrical and Electronic Engineering, COMPEL, vol. 32, no. 5, pp. 1552 - 1566, 2013.

IX. BIOGRAPHIES

Christelle Piantsop Mbo'o was born in 1982 in Douala, Cameroon. She received her Dipl.-Ing. degree in electrical engineering in 2008 from RWTH Aachen University, Germany. Since 2009 she has been a researcher at the Institute of Electrical Machines (IEM). Her research interests include analysis and design of electrical machines.

Thomas Herold was born in 1977 in Daun, Germany. He received the Dipl. -Ing. degree in electrical engineering in 2007 from RWTH Aachen University, Germany. After that he became a member of staff (research associate) at the Institute of Electrical Machines, RWTH Aachen University. Since 2010 he has been working as chief engineer of the institute. His main field of research is drive-train modelling and simulation, propulsion control, and system identification.

Dr. Kay Hameyer (FIET, SMIEEE) received his M.Sc. degree in electrical engineering from the University of Hannover and his Ph.D. degree from the Berlin University of Technology, Germany. After his university studies he worked with the Robert Bosch GmbH in Stuttgart, Germany as a Design Engineer for permanent magnet servo motors and vehicle board net components. Until 2004 Dr. Hameyer was a full Professor for Numerical Field Computations and Electrical Machines with the KU Leuven in Belgium. Since 2004, he is full professor and the director of the Institute of Electrical Machines (IEM) at RWTH Aachen University in Germany. 2006 he was vice dean of the faculty and from 2007 to 2009 he was the dean of the faculty of Electrical Engineering and Information Technology of RWTH Aachen University. His research interests are numerical field computation and optimisation, the design and controls of electrical machines, in particular permanent magnet excited machines, induction machines and the design employing the methodology of virtual reality. Since several years Dr. Hameyer's work is concerned with the development of magnetic levitation for drive systems, magnetically excited audible noise in electrical machines and the characterisation of ferro-magnetic materials. Dr. Hameyer is author of more then 250 journal publications, more then 500 international conference publications and author of 4 books. Dr. Hameyer is a member of VDE, IEEE senior member, fellow of the IET.